Melt Spinning of Fibers: Effect of Air Drag

Y. D. KWON and D. C. PREVORSEK, *Chemical Research Center, Allied Chemical Corporation, Morristown, New Jersey 07960*

Synopsis

Experimental measurements of the magnitude of air drag on the filament and the air velocity profile around the filament in the spinning and drawing down of a fiber filament in the surrounding of stagnant air are reported. The results are examined in comparison with the existing theoretical correlations that have been used in the studies of the spinning processes. The experimental values of the air drag are found to be larger than the values based on the existing correlations to such an extent that, in some cases of past studies, the air drag effect on the filament tension may have been underestimated.

INTRODUCTION

From the rheological point of view, a typical melt spinning process poses a transient, nonlinear, nonisothermal problem which is "beyond our current capability of analysis."[1] Nevertheless, many authors took the simplified approaches and investigated the relationship between the operating variables and the thinning and cooling profiles of the filament in the spinway (for example, Ziabicki[2]). The analyses involve estimate of the "rheological force" F_{rheo} as a function of the position x (measured down from the spinneret) in the spinway using the take-up tension F_L measured at the take-up point $x = L$ and accounting for the effect of gravitational force F_{grav}, inertia force F_{inert}, and the air drag F_{drag} by the relation

$$F_{\text{rheo}}(x) = F_L + F_{\text{grav}}(x) - F_{\text{drag}}(x) - F_{\text{inert}}(x) \tag{1}$$

where

$$F_{\text{grav}}(x) = \int_x^L \rho g \frac{\pi d^2(x)}{4} dx \tag{1a}$$

$$F_{\text{drag}}(x) = \int_x^L \sigma_f \pi d(x) dx \tag{1b}$$

$$F_{\text{inert}}(x) = M[U_f(L) - U_f(x)] \tag{1c}$$

ρ is density of the filament, g is gravitational constant, $d(x)$ is filament diameter at position x, σ_f is shear stress in air on the filament surface, M is mass rate of filament, and U_f is filament velocity.

Given the filament diameter profile $d(x)$, estimate of $F_{\text{grav}}(x)$ and $F_{\text{inert}}(x)$ is straightforward, but estimate of $F_{\text{drag}}(x)$ is not so simple. The shear stress σ_f is usually expressed by

$$\sigma_f = c_f \frac{\rho U_f^2}{2} \tag{2}$$

Jurnal of Applied Polymer Science, Vol. 23, 3105–3122 (1979)

0021-8995/79/0023-3105$01.00

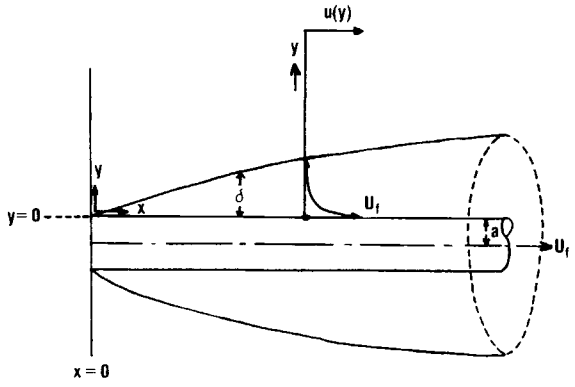

Fig. 1. Boundary layer over a moving cylindrical surface.

where c_f is a friction factor. So, the not-so-simple problem here is to find the value of c_f as the function of the related variables.

Perhaps because of the fact that c_f cannot be obtained simply, authors handled the matter in different ways. Some simply neglected the air drag, believing that its magnitude is just insignificant relative to the magnitude of F_{rheo} (for example, Cernia et al.[3]). On the other hand, some authors accounted for the effect of air drag on F_{rheo} and showed that F_{drag} can be as large as one third of F_{rheo}.[4]

As for those authors who accounted for the effect of air drag on F_{rheo}, many of them used the laminar boundary layer correlations of Sakiadis.[5] Although there are experimental data reported on the air drag to moving filaments[6] that indicate that the actual air drag may be larger than the values predicted by Sakiadis' correlation, not much attention has been paid to the data.

From the fact that many authors proceeded to use the values of F_{rheo} obtained through the above-mentioned estimating procedure, it is obvious that the results obtained, such as the elongational viscosity (or tensile viscosity), are subject to the uncertain error related to the magnitude of F_{drag}. Thus, Bankar et al.[1] expressed concern for the possible underestimate of the air drag effect on the values of F_{rheo}.

This uncertain situation prompted the present authors to attempt the experimental measurements of the air drag and the air velocity profile in the boundary layer around the moving filament. By comparative examination of the experimental data with the existing experimental data and the existing theoretical correlations, the authors hope to establish better understanding of the magnitude of the air drag in the spinning processes.

PREVIOUS WORK ON THEORY

The problem under consideration is related to the axisymmetrical boundary layer over a long thin cylinder as depicted in Figure 1. In the comparative examination of experimental data with the existing data and existing theoretical correlations, it is useful to define the Reynolds numbers and the drag coefficient as follows:

$$Re_x = U_f x/\nu_a \tag{2a}$$

$$Re_a = U_f a/\nu_a \tag{2b}$$

$$C_D = D/\rho_a U_f^2 aL \tag{2c}$$

TABLE I
Values of Re_x and Re_a as Functions of x and a in 25°C Air[a]

Filament diameter d, cm	Filament radius a, cm	Nylon 6 filament denier	Filament speed U_f, cm/sec	Re_a	Position x, cm	Re_x
0.002	0.001	3.3	10	0.0637	10	6.37×10^2
					100	6.37×10^3
			1000	6.369	10	6.37×10^4
					100	6.37×10^5
0.01	0.005	82.5	10	0.318	10	6.37×10^2
					100	6.37×10^3
			1000	31.85	10	6.37×10^4
					100	6.37×10^5
0.02	0.01	330	10	0.637	10	6.37×10^2
					100	6.37×10^3
			1000	63.7	10	6.37×10^4
					100	6.37×10^5

[a] $\rho_a = 0.00118$ g/cc; $\nu_a = 0.157$ cm^2/sec.

where ν_a is kinematic viscosity of air, a is filament radius, D is total drag force, L is length of the filament, and ρ_a is density of air.

In order to establish the ranges for Re_x and Re_a in which fiber spinning is carried out, we show in Table I values of these two parameters for various values of U_f, a, and x at 23°C. For example, when a 4-denier filament is spun at a take-up speed of 5000 ft/min through a 10-ft-high spinway, the corresponding $Re_a \approx 16$ and $Re_{x_{max}} \approx 2 \times 10^6$. These conditions represent a typical industrial spinning process. Many experimental spinning processes are conducted under conditions which approach the following case: filament denier = 1500, take-up speed = 200 ft/min, spinway height = 6.7 ft. For this case $Re_a \approx 3.2$ and $Re_{x_{max}} \approx 1.2 \times 10^5$.

For the purpose of this study it is necessary to establish whether the flow in the boundary layer is laminar or turbulent. For a boundary layer on a continuous flat plate surface, the transition from a laminar to turbulent boundary layer is believed to occur at $Re_x = 5 \times 10^5$.[7] This means that for most cases of industrial and experimental spinning, the boundary layer is laminar in the upper part of the spinway and turbulent in the lower part. Therefore, in an analysis of the effect of air drag on the filament tension in spinning processes, it is necessary to consider both the laminar and turbulent boundary layers.

Sakiadis' results which were used by many authors were obtained for the laminar boundary layer. This approach is similar to that of Pohlhausen[8] which was also followed by Glauert and Lighthill.[9] These authors expressed the boundary layer velocity profile by

$$\frac{u(y)}{U_f} = 1 - \frac{1}{\beta(x)} \ln\left(1 + \frac{y}{a}\right) \tag{3}$$

where y is transversal position measured from the filament surface, $u(y)$ is air velocity at position y, and $\beta(x)$ is boundary layer parameter dependent on x. The parameter $\beta(x)$ is given as a function of log ξ where

$$\xi = 4\sqrt{\frac{\nu_a X}{U_f a^2}} \tag{4}$$

With the $\beta(x)$, the boundary layer thickness $\delta(x)$ and the shear stress at the filament wall σ_f can be calculated by

$$\frac{\delta(x)}{a} = e^{\beta(x)} - 1 \tag{5}$$

$$\sigma_f(x) = \frac{\mu_a U_f}{a\beta(x)} \tag{6}$$

here μ_a is the air viscosity.

For the turbulent boundary layer over a long thin cylinder, Sakiadis[5] attempted to use the boundary layer velocity profile over a flat plate, i.e.,

$$\frac{u(y)}{U_f} = 1 - \left(\frac{y}{\delta}\right)^{1/7} \tag{7a}$$

and the shear stress correlation of the flat surface boundary layer

$$\frac{\sigma_f}{(\rho_a/2)U_f^2} = C_f = 0.045\left(\frac{\nu_a}{U_f\delta}\right)^{1/4} \tag{7b}$$

But the author concluded that the results obtained were not satisfactory.

More recently, White[10] carried out an analysis of the problem using a modified form of the law of the wall deduced by Rao.[11] Rao's approach is to define two variables:

$$u^+(y) = \frac{u(y)}{\sqrt{\sigma_f/\rho_a}} \tag{8a}$$

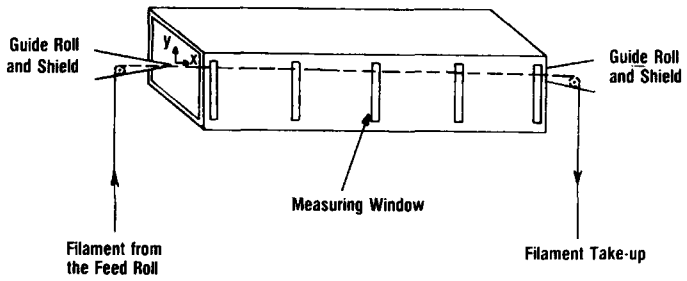

Fig. 2. Experimental setup for the measurement of air velocity profile in the boundary layer.

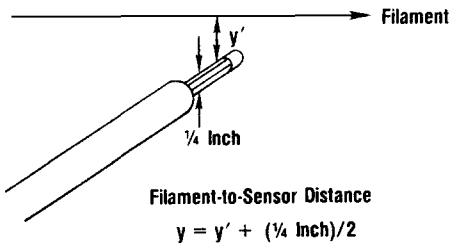

Fig. 3. Sensor of the anemometer.

$$Y = \frac{a\sqrt{\sigma_f/\rho_a}}{\nu_a} \ln\left(1 + \frac{y}{a}\right) \tag{8b}$$

and correlate $u^+(y)$ against ln Y. All the experimental data available at that time[11-13] could be correlated by this equation.

White's analysis[10] leads to the following approximate formula:

$$C_D = 0.0015 + \left[0.3 + 0.015\left(\frac{L}{a}\right)^{0.4}\right] R_L{}^{-1/3} \tag{9a}$$

for $10^6 \leq Re_L \leq 10^9$ and $L/a \leq 10^6$

$$C_D = \frac{4}{Re_a}\left[\frac{1}{G} + \frac{1.5772}{G^2} + \cdots\right] \tag{9b}$$

where $G = \ln(4Re_L/Re_a{}^2)$ for $G \leq 6$ and $Re_a \leq 20$.

$$c_f = 0.0015 + \left[0.2 + 0.016\left(\frac{y}{a}\right)^{0.4}\right] Re_x \tag{9c}$$

for $10^6 \leq Re_x \leq 10^9$

$$c_f = \frac{4}{Re_a}\left[\frac{1}{G} + \frac{0.5772}{G^2} + \cdots\right] \tag{9d}$$

for $Re_a < 25$. Expressions (9b) and (9d) are based on the asymptotic series solution of Glauert and Lighthill.[9]

White also compared the experimental values of C_D including those of Selwood.[6] Selwood's results were the only data obtained with cylindrical filaments of textile fiber dimensions. It was pointed out that Selwood's values were much larger than those predicted by theories of White, Glauert, and Lighthill. It was suggested that the discrepancy may be attributed to "such unknown matters as roughness effects, incorrect or varying fiber diameters and possible tensiometers discrepancies."

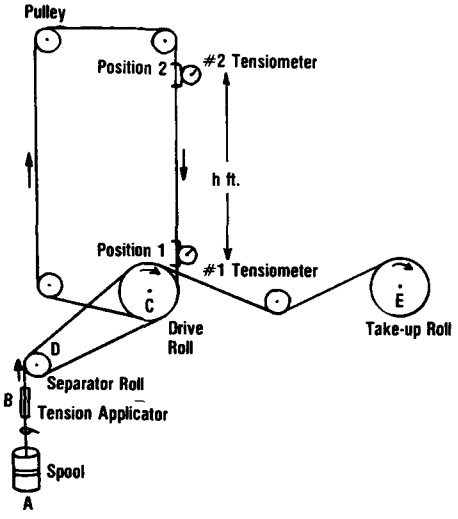

Fig. 4. Experimental setup for measuring air drag around a moving filament.

In another study, Cebeci[14] solved the boundary layer equations by finite difference method. The resulting velocity profile agreed with the Rao's law of the wall[11] described by eqs. (8a) and (8b).

In applying these theoretical and experimental results to estimate the air drag in melt spinning one must be concerned with the following facts:

1. All the authors recognized that the friction factor rises as the transverse curvature increases. Yet no investigation except those by Selwood[6] and Anderson and Stubbs[15] really considered the case of thin filaments. Thus, there is the possibility of unreasonable extrapolation when the results obtained with larger cylinders are applied to the thin filaments.
2. The theories developed are for the constant diameter cylinders whereas the spinning process deals with varying cylinder diameter. So the results can be applied only to the section where the filament diameter remains approximately constant.
3. The theories assume the cylinder to be "stationary" holding the fixed spatial position. In spinning, amplitude of the filament swaying usually exceeds filament diameter. Therefore, the air drag in spinning is not the same as that on a stationary cylinder.

Based on these considerations it appeared desirable to conduct experimental measurements of air drag on the filaments under conditions similar to those in actual spinning. In this article we review the results of a study where air drag on moving filaments was measured under conditions similar to those in melt spinning of synthetic fibers.

EXPERIMENTAL

Measurement of Velocity Profile in the Boundary Layer

The experimental setup used for the measurement of the boundary layer velocity profile of air around a moving filament is shown in Figure 2. A filament is unwound from a spool and fed into the measuring tunnel by means of a speed-controlled feed roll. The tunnel used in the experimental measurements had a dimension of 2 ft × 2 ft × 8 ft. One of the side walls is equipped with windows through which the anemometer (Fig. 3) can be inserted and positioned at a desired distance from the filament. At the exit end of the tunnel, the filament is guided through the guide roll and taken up by a take-up roll. Both of the guide rolls are shielded so that the stirring of air by the rotating rolls is minimized. In the measurement of velocity profile, all but one of the measuring windows being used are sealed. After setting the filament velocity to a desired level, the air velocity around the filament is measured as the function of radial distance at each of the axial positions. This tunnel was needed to minimize the effect of air current in the room on the velocity profile in the boundary layer.

The air velocity was measured by use of a thermoanemometer (Alnor Thermo-Anemometer Type 8500K No. 1498, manufactured by Alnor Instrument Co., Chicago, Ill). The sensing element of this anemometer has a protection frame as shown in Figure 3. In determining the filament-to-sensor distance, therefore, half of the thickness of the protection frame was added to the filament to frame distance (Fig. 3).

TABLE II
Results of the Measurements of Boundary Layer Velocity Profile[a]

	Boundary layer velocity, ft/min				
y, in.	x = 1/6 ft	2 ft	4 ft	6 ft	8 ft
	Run 1: 20 denier, diameter 0.0049 cm, U_f = 305 ft/min				
1/8	<9–12	20–37	25–40	30–40	30–43
1/4	<9		13–30	10–25	15–25
3/8		15–25	< 9–25	13–30	10–20
1/2		12–21	< 9–21	< 9–20	< 9–16
5/8			< 9–15	< 9–20	< 9–15
7/8		< 9–17	< 9–16	< 9–15	< 9–14
1 1/8		< 9–13	< 9–15	< 9–15	< 9–13
2 1/8		< 9	< 9–10		
4 1/8					
	Run 2: 20 denier, diameter 0.0049 cm, U_f = 615 ft/min				
1/8	12–28	35–60	40–60	35–60	30–50
1/4	< 9–23	15–45	40–55	30–55	22–38
3/8	< 9–18	15–33	20–40	22–36	18–28
1/2	< 9–15	12–30	20–35	25–34	18–30
5/8	< 9–14	< 9–25	20–35	14–28	17–28
7/8		< 9–20	10–25		15–25
1 1/8		< 9–19	10–20	13–22	12–21
2 1/8		< 9–11			11–18
4 1/8		< 9	< 9–15	< 9–14	< 9–11
	Run 3: 20 denier, diameter 0.0049 cm, U_f = 915 ft/min				
1/8	18–34	45–65	55–70	50–70	40–60
1/4	13–20	38–58	40–60	35–60	27–42
3/8	10–11	32–48	25–60	25–40	20–30
1/2	< 9–10	20–35	20–40	20–35	17–35
5/8		17–30	15–36	20–35	22–30
7/8	< 9	15–25	13–26	15–30	20–31
1 1/8		9–21	9–20	< 9–20	19–30
2 1/8		< 9–10	< 9–13	< 9	
4 1/8		< 9	< 9–10		< 9
	Run 4: 20 denier, diameter 0.0049 cm, U_f = 1210 ft/min				
1/8	45–80	60–85	68–85	75–95	70–85
1/4	18–35	50–70	50–70	65–80	50–70
3/8	12–20	35–58	40–65	40–58	28–48
1/2	< 9–16	30–55	25–50	35–55	25–40
5/8	< 9–14	20–45	30–42	30–47	
7/8	< 9	12–25	15–33	20–40	22–32
1 1/8		10–22	< 9–28	13–30	18–30
2 1/8		< 9–11	< 9–11	10–20	12–21
4 1/8			< 9	< 9	< 9–14
	Run 5: 200 denier, diameter 0.0155 cm, U_f = 300 ft/min				
1/8	17–23	43–70	40–70	30–52	35–58
1/4	< 9	29–47	25–50	25–45	25–37
3/8		11–20	14–30	18–35	13–30
1/2		< 9	< 9–25	16–30	9–23
5/8			< 9–22	< 9–22	12–25
7/8			< 9–18	< 9–17	< 9–18

TABLE II. *Continued.*

y, in.	Boundary layer velocity, ft/min				
	x = 1/6 ft	2 ft	4 ft	6 ft	8 ft
Run 1: 20 denier, diameter 0.0049 cm, U_f = 305 ft/min					
1 1/8			< 9–15	< 9–15	< 9–16
2 1/8			< 9	< 9	< 9–10
4 1/8					< 9
Run 6: 200 denier, diameter 0.0155 cm, U_f = 925 ft/min					
1/8	35–64	85–105	90–110	80–100	80–100
1/4	20–42	55–85	70–90	62–85	60–80
3/8	12–16	45–63	50–70	50–72	48–70
1/2	10–16	35–60	35–60	40–58	38–60
5/8	9–16	25–50	35–55	35–60	35–50
7/8	9–13	20–40	18–45	30–50	25–40
1 1/8		14–35	25–38	25–45	25–45
2 1/8		10–16	15–30	13–29	10–30
4 1/8			< 9–12	< 9–12	< 9–15

[a] The pairs of values indicate the lower and upper bounds of the fluctuations of observed velocity. < 9 means that the lower bound is below the lower limit of the anemometer, which is 9 ft/min. U_f = filament velocity, x = axial position, y = radial position.

The accuracy of the anemometer was checked by installing a rotameter before a cylindrical duct. A stream of air was passed through this duct at a desired flow rate indicated by the rotameter. The air velocity at various radial positions in the cross section of the cylindrical duct at the outlet side was measured by the anemometer and the total flow rate was calculated by integrating the air velocity profile. The values obtained by integration of the radial velocity profile matched the value indicated by the rotameter within a maximum discrepancy of 4%.

Measurement of Air Drag Around a Filament Moving in Air

The setup used for the measurement of air drag on moving filament is shown in Figure 4. A filament of known diameter is unwound from a spool (A), guided through a tension applicator (B), wrapped several times over the drive roll (C) and separator roll (D) to prevent slippage, guided upward to a pair of pulleys which are installed at h ft above the drive roll (C), guided down back to the drive roll on which it is wrapped around once, and finally taken up by means of a take-up roll (E). This filament path was used to maintain the filament tension at a preselected level and to minimize the fluctuation of the tension during the measurement. The filament tension was adjusted by means of the tension applicator before the drive roll and by the tension adjuster of the take-up machine.

The measurements were carried out by moving the filament at a desired velocity and tension. Two tensiometers, #1 (at the lower side) and #2 (at the upper side), are first inserted adjacent to each other at position 1 (Fig. 4) with the #2 tensiometer positioned at the upper side, and the readings of the two tensiometers are taken. Next, the tensiometer #2 is moved to position 2 and readings of the two tensiometers are taken again. From these readings, the air drag on the filament segment between the positions 1 and 2 is calculated by eq. (10). The tensiometers used were Type Ten-2K made by N. Zivy and Cie, S. A. Schweiz.

A force balance yields the following relationship between the air drag and the above described readings of the tensiometers:

$$D_a - w_f = (T_L - T_U)_2 - (T_L - T_U)_1 \tag{10}$$

where D_a is the air drag on the filament segment between positions 1 and 2, w_f is the weight of the same filament segment, T is the tensiometer readings, with the subscripts L and U indicating whether the tensiometer is the one at the lower side (#1) or the one at the upper side (#2), respectively, and the subscripts 1 and 2 indicate the position of the tensiometer #2 (at the upper side) at the time of reading. The value of w_f is determined from the denier and length of the filament. Thus, the air drag D_a can be obtained from Eq. (10).

The advantage of this two-tensiometer measuring system is that the absolute errors of individual tensiometers are canceled out by the subtractions indicated in eq. (10).

RESULTS

Boundary Layer Velocity Profiles

The experimental measurements were carried out with 20 denier, 70 denier, and 200 denier nylon 6 filaments. The filament velocities were varied from 300 ft/min to 1200 ft/min. Pertinent data are listed in Table II. In Figure 5 are shown the velocity profiles determined in run 6. For comparison we included (a) the velocity profile based on the boundary layer equation for flat surface and (b) the velocity profile calculated from the equation for laminar boundary layer around a cylinder used by Sakiadis. Both theoretical velocity profiles show boundary layer thicknesses which are much smaller than the observed one.

In the figure, we notice that the observed velocity values show fluctuations within certain ranges at each of the measuring points. To check if this fluctu-

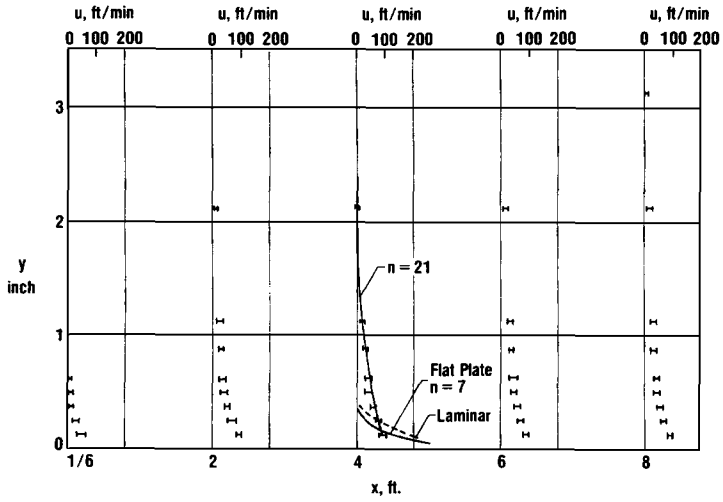

Fig. 5. Boundary layer velocity profiles (run 6). U_f = 925 ft/min, 200 denier, diameter = 0.0155 cm.

ation is due to any interference from outside, the filament motion was frequently stopped while the anemometer was kept at the measuring point. Invariably, the anemometer registered a zero value in such cases. The fluctuations occur in a periodic manner, with the period fluctuating between 2 and 4 sec.

Air Drag

The experimental measurements of air drag were carried out with 20 denier, 70 denier, and 200 denier filaments. Velocities of the filaments were varied from 300 ft/min to 1200 ft/min. Results of the measurements are summarized in Table III and in Figure 6. For each measurement, seven readings were taken and the values were averaged to obtain the values shown.

DISCUSSION

On the Air Velocity Profile in the Boundary Layer

Figure 5 shows the experimentally measured air velocity profile in the boundary layer. It is plotted as the function of y and x. The fluctuation of air velocity observed is indicated by the symbol I to show the range of fluctuation. Although we are not certain about the origin of these velocity fluctuations, we suspected that they are caused by filament swaying. Consequently, the filament position is not "stationary" as assumed in the theoretical analyses.

Consider now the air velocity profile at $x = 4$ ft for the case shown in Figure 5 (run 6) and compare this result with the air velocity profile calculated by eq. (3). The value of Re_x given by eq. (2a) is 46.4, and therefore the boundary layer must be laminar. The ξ of eq. (4) is 103.8, and using the numerical correlation of Sakiadis, we obtain

$$\delta(x)/a = 104.1 \qquad \beta(x) = 4.65 \tag{11}$$

Using this value of $\beta(x)$ in eq. (3), the air velocity is calculated as shown in Figure 5 by the dotted line labeled "laminar."

Comparing the measured the calculated laminar velocity profiles we see that (1) the actual boundary layer thickness is at least seven times thicker; (2) the actual velocity profile is much flatter than the calculated velocity profile.

Also for comparison, we show a turbulent velocity profile over a flat plate calculated using the procedure of Sakiadis. The profile is indicated in Figure 5 by "flat plate." Note that the calculated boundary layer thickness is much smaller than the experimental one.

The actual velocity profile can be approximated well by

$$\frac{u(y)}{U_f} = 1 - \left(\frac{y}{\delta}\right)^{1/n} \tag{12}$$

with $n = 21$ and $\delta = 2.0$ in. Note that eq. (12) has the same form as eq. (7a), except for the value of index n.

When the boundary layer velocity profile $u(y)$ at axial position x is given, the total drag on the filament from $x = 0$ to the position x can be calculated in terms of the momentum integral.

TABLE III
Experimental Data of Air Drag Measurements with Nylon 6 Filaments

Run no.	Denier	Diameter cm	Height, ft	Velocity, ft/min	$(T_L - T_U)_2$ (average)[a]	$(T_L - T_U)_1$ (average)[a]	w_f, g (calcd)	D_a, g
1	20	0.0049	20.5	313	2.71	2.71	0.0138	0.014
2				610	2.95	2.92		0.044
3				940	4.16	4.085		0.089
4				1230	4.74	4.62		0.134
5			11.0	1230	4.67	4.62	0.008	0.058
6	70	0.0092	20.5	290	0.98	1.0	0.0483	0.028
7				595	0.95	0.9		0.098
8				890	1.86	1.74		0.171
9				1180	1.98	1.79		0.258
10	200	0.0155	20.5	270	0.964	1.05	0.138	0.052
11				620	1.03	1.0		0.162
12				760	1.2	1.1		0.238
13				1170	1.40	1.10		0.438

[a] Average of seven readings.

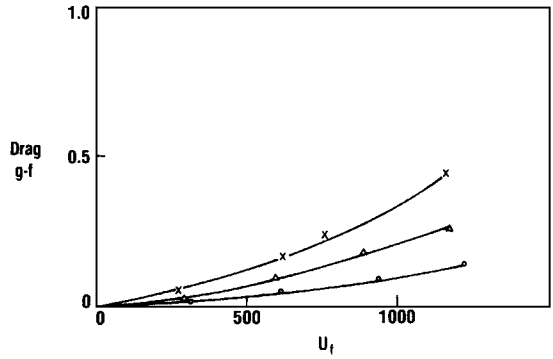

Fig. 6. Air drag measurements: (×) 200 denier (diameter = 0.0155 cm); (△) 70 denier (diameter = 0.0092 cm); (○) 20 denier (diameter = 0.0049 cm); U_f filament velocity, ft/min; height, 20½ ft, filament, nylon 6.

$$D(x) = \int_0^{\delta(x)} 2\pi\rho(a + y)u^2(y)\, dy \tag{13}$$

Using the $u(y)$ given by eq. (12), eq. (13) becomes

$$D(x) = 2\pi\rho_a U_f{}^2[(\alpha_n a\delta(x) + \gamma_n \delta^2(x)] \tag{14}$$

with

$$\alpha_n = 1 - \frac{2n}{2n+1} + \frac{n}{n+2}$$

$$\gamma_n = \frac{1}{2} - \frac{2n}{2n+1} + \frac{n}{2n+2} \tag{15}$$

In Sakiadis' derivation for laminar boundary layer, $D(x)$ is given by

$$D(x) = \pi a^2 \rho_a U_f^2 \left[\frac{e^{2\beta} - 1}{2\beta^2} - \frac{1}{\beta} - 1\right] \tag{16}$$

So, from eqs. (14) and (16), we can determine the ratio of the drag based on the actual measured velocity profile and the drag calculated from the laminar theory. The ratio R is

$$R = \frac{2[\alpha_n a\delta(x) + \gamma_n \delta^2(x)]}{a^2[(e^{2\beta} - 1)/2\beta^2 - 1/\beta - 1]} \tag{17}$$

For the case under the consideration, the ratio R is found to be 6.17. Thus, from the result of the velocity measurement, we find that the actual drag is considerably larger than the value calculated from the laminar boundary layer theory of Sakiadis.

For the cases of 20 denier and 70 denier filaments, n is empirically found to be approximately 28 and 25, respectively. Thus, as shown in Figure 7, the index n is increasing with the decrease of the filament radius in the range of the radii examined.

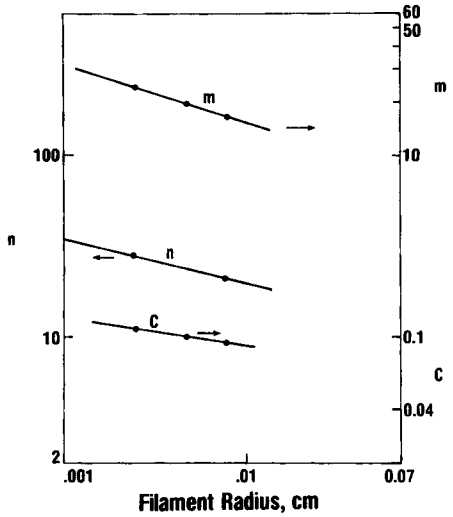

Fig. 7. Boundary layer parameters vs filament radius.

Drag

It was seen in the previous section that the boundary layer velocity profile around a moving thin filament is such that the drag may be larger than the values calculated from theory. Therefore, in this section we examine the actual drag data generated by the present authors together with the data of Selwood.

A convenient way of comparing the data is to calculate the drag coefficient C_D as defined by eq. (2c) and compare it with the value of C_D calculated by eqs. (9a) or (9b). Table IV shows the results of this comparisons. The observations are:

a. All the experimental values of the drag obtained with the thin fiber filaments are considerably larger than the values obtained with the formula of Eq. (9a) or (9b).

b. Even when Re_L is well over the transition point into the turbulent region, eq. (9b) gives values which are consistently close to the experimental values.

c. The ratio R increases with the increase of Re_L or Re_a, and it increases with the decrease in the calculated C_D. The plot of the ratio R against $C_{D_{cal}}$ is shown in Figure 9. Within the range of variables covered by these experiments, the correlation of Figure 9 can be used for the calculation of C_D. Note the large difference between calculated and experimental values of C_D.

We attribute the difference between the experimental values and calculated values of C_D to filament swaying. As a result, the effective diameter of a moving filament is larger than the true filament diameter. The degree of swaying is expected to increase with the increase of filament length and filament speed, and this is the trend seen with the experimental data.

Empirical Correlations for Interpolation of the Data

We showed that the index n of eq. (12) increases monotonically with the decrease of the filament radius a (see Fig. 7). So, if the value of filament radius a is given, the corresponding value of the index n can be determined by inter-

TABLE IV
Comparison of experimental values of C_D with Those Calculated by Eq. (9a) or (9b)[a]

Date[a] source	Run no.	Denier	a, cm	L, cm	U_f, cm/sec	D, g force	C_D, exp	Re_L	Re_a	$G = \ln 4Re_L/Re_a^2$	L/a
Kwon and Prevorsek	1	20	.00245	624.8	159	.014	.0957	6.33×10^5	2.48	12.9	2.55×10^5
	2			624.8	310	.044	.0791	1.23×10^6	4.84	12.3	2.55×10^5
	3			624.8	477.5	.089	.0675	1.9×10^6	7.45	11.8	2.55×10^5
	4			624.8	624.8	.134	.0593	2.48×10^6	9.75	11.6	2.55×10^5
	5			335.2	624.8	.058	.0479	1.33×10^6	9.75	10.94	1.37×10^5
	6	70	.0046	624.8	147.3	.028	.119	5.86×10^5	4.32	11.7	1.36×10^5
	7			624.8	302	.098	.0989	1.2×10^6	8.85	11.0	1.36×10^5
	8			624.8	452.1	.171	.077	1.8×10^6	13.3	10.6	1.36×10^5
	9			624.8	599.4	.258	.0661	2.4×10^6	17.6	10.3	1.36×10^5
	10	200	.00775	624.8	137.1	.052	.1511	5.46×10^5	6.77	10.77	8.06×10^4
	11			624.8	315	.162	.0892	1.25×10^6	15.55	9.94	8.06×10^4
	12			624.8	386	.238	.0872	1.54×10^6	19.1	9.74	8.06×10^4
	13			624.8	594.4	.438	.0677	2.36×10^6	29.3	9.3	8.06×10^4
Selwood	1	6	.00135	2000	500	.47	.184	6.37×10^6	4.3	14.1	1.48×10^6
	2			2000	1000	1.08	.106	1.27×10^7	8.60	13.4	1.48×10^6
	3			2000	1500	2.02	.088	1.91×10^7	12.9	13.0	1.48×10^6
	4			2000	2000	2.35	.0576	2.55×10^7	17.2	12.8	1.48×10^6
	5	15	.0021	2000	500	0.45	.113	6.37×10^6	6.69	13.3	9.52×10^5
	6			2000	1000	1.07	.0674	1.27×10^7	13.4	12.6	9.52×10^5
	7			2000	1500	1.9	.0532	1.91×10^7	20.1	12.2	9.52×10^5
	8			2000	2000	2.7	.0425	2.55×10^7	26.8	11.9	9.52×10^5
	9	60	.0042	2000	500	0.73	.0919	6.37×10^6	13.4	11.9	4.76×10^5
	10			2000	1000	1.7	.0535	1.27×10^7	26.8	11.2	4.76×10^5
	11			2000	1500	2.5	.0350	1.91×10^7	40.1	10.8	4.76×10^5
	12			2000	2000	3.9	.0307	2.55×10^7	53.5	10.5	4.76×10^5

TABLE IV. Continued.

$C_{D_{calc}}$		$C_{D_{exp}}/C_{D_{calc}}$	
Eq. (9a)	Eq. (9b)	Eq. (9a)	Eq. (9b)
.0304	.140	3.146	.684
.0246	.0761	3.21	1.039
.0215	.0514	3.13	1.31
.0198	.0403	2.99	1.47
.0197	.043	2.43	1.15
.0253	.0895	4.68	1.33
.0203	.0469	4.88	2.11
.0179	.0327	4.3	2.36
.0164	.0254	4.02	2.60
.022	.063	6.86	2.4
.017	.03	5.23	2.97
.016	.025	5.44	3.48
.0141	.0171	4.81	3.95
.0269	.0731	6.84	2.51
.0217	.0387	4.88	2.74
.0191	.0267	4.6	3.3
.0175	.0205	3.29	2.81
.0231	.0505	4.91	2.25
.0186	.0268	3.62	2.51
.0165	.0185	3.23	2.87
.0151	.0143	2.82	2.98
.0182	.0285	5.04	3.22
.0148	.0153	3.62	3.51
.0131	.0106	2.67	3.30
.0120	.0082	2.55	3.74

[a] 25°C; $\rho_a = 0.00118$ g/cc; $\nu_a = 0.157$ cm^2/sec.

polation from Figure 7. Then, if we know $\delta(x)$, the drag $D(x)$ can be calculated by eq. (13). However, in most cases $\delta(x)$ is not known. In this case the following procedure is used to estimate $\delta(x)$: We rewrite eq. (7b) in the form

$$\frac{\sigma_f(x)}{(\rho_a/2)U_f^2} = C_f = c\left(\frac{\nu_a}{U_f\delta(x)}\right)^{1/m} \tag{18}$$

and let c and m vary with the filament radius a. Combining eqs. (18), (12), and (13) and defining

$$\zeta(x) = \frac{\delta(x)}{a} \tag{19}$$

we obtain

$$\frac{m}{m+1}\alpha_n\zeta^{(m+1)/m} + \frac{m}{2m+1}2\gamma_n\zeta^{(2m+1)/m} = \frac{C}{2}\frac{x}{a}\left(\frac{\nu_a}{U_f a}\right)^{1/m} \tag{20}$$

Given a set of the values of c, m, and n, eq. (20) can be solved to give ζ and hence $\delta(x)$.

The data of Tables II and III were used in combination with eq. (20) to determine the best fitting values of m and c as the function of a. The results are shown in Figure 7. Using these values of m, c, and n we regenerated the velocity

profile and air drag. The results are compared with the original data in Table V and Figure 8. In general, the agreement is good. Thus, in the range of the variables experimented, eqs. (12) and (18) can be used for the calculation, by interpolation, of the velocity profile in the boundary layer and the shear stress at the filament wall.

Effect of the Air Drag in Melt Spinning

Applying the above results, we examine two cases of spinning experiments reported in literature and determine error associated with incorrect treatment of air drag effect.

First, we consider the results of Cernia et al.[3] who neglected the air drag in calculating the elongational viscosity from the take-up tension. In run C, 80 denier filament was picked up at a take-up speed of 700 m/min, and the take-up tension was 500 dynes. Assuming that for about half of the spinway (80 cm) the filament diameter was equivalent to 80 denier, the air drag to that segment of filament based on the correlation of Figure 9 is 127 dynes ($Re_L = 5.9 \times 10^5$, $Re_a = 33.4$, $L/a = 1.78 \times 10^4$, $G = 10$, $C_{D_{\text{calc}}} = 0.0219$, $C_{D_{\text{exp}}} = 0.07$). This is about 25% of the take-up tension of 500 dynes. Thus, the elongational viscosity calculated at the upper section of the filament should be about 25% lower than the values reported.

Next we consider the case of nylon 6 spinning studied by Ishibashi et al.[16] The authors used Sakiadis' results[5] in accounting for the effect of air drag. Taking run 3, the filament diameter is about 0.008 cm for the lower 600-cm segment out of about 680 cm of total spinway. The take-up velocity was 100 cm/sec and, according to Figure 7 of the reference, the air drag is estimated to be approximately 0.12 g force. The value of air drag computed by the correlation of Figure 9 is 0.561 g force ($Re_L = 3.8 \times 10^6$, $Re_a = 25.4$, $L/a = 1.5 \times 10^5$, $G = 10$, $C_{D_{\text{calc}}} = 0.01844$, $C_{D_{\text{exp}}} = 0.0618$). Even by using the calculated value of C_D, the drag is found to be about 0.167 g force, which is almost 40% larger than the value obtained with the Sakiadis correlation. The value of 0.561 g force is larger than the take-up tension, which was about 0.35 g force. Thus, in this case, the value

TABLE V
Comparison of Experimental Air Drag with the Values Calculated Through Interpolation Using Eqs. (12), (18), and (20)

Denier	Diameter, cm	Velocity, ft/min	Drag (exp), g force	Drag (calculated), g force
20	0.0049	313	0.014	0.0104
		610	0.044	0.0404
		940	0.089	0.0896
		1230	0.134	0.1574
70	0.0092	290	0.028	0.0164
		595	0.098	0.0633
		890	0.171	0.1395
		1180	0.258	0.245
200	0.0155	270	0.052	0.0236
		620	0.162	0.0909
		760	0.238	0.199
		1170	0.438	0.3496

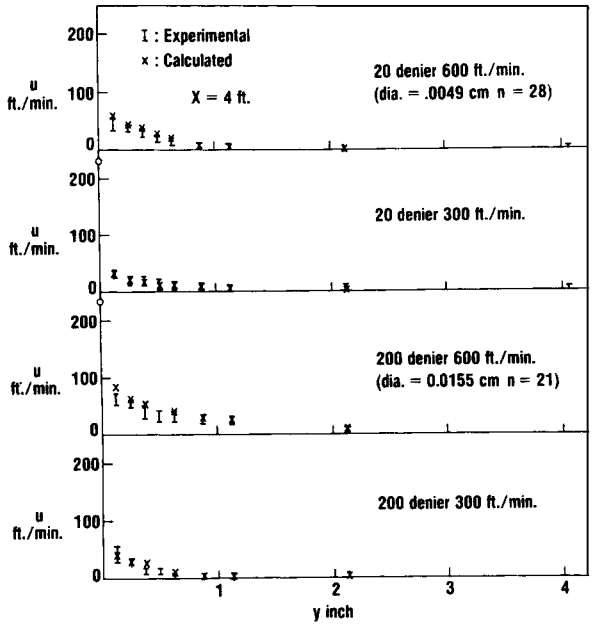

Fig. 8. Comparison of boundary layer velocity profiles, experimental and calculated.

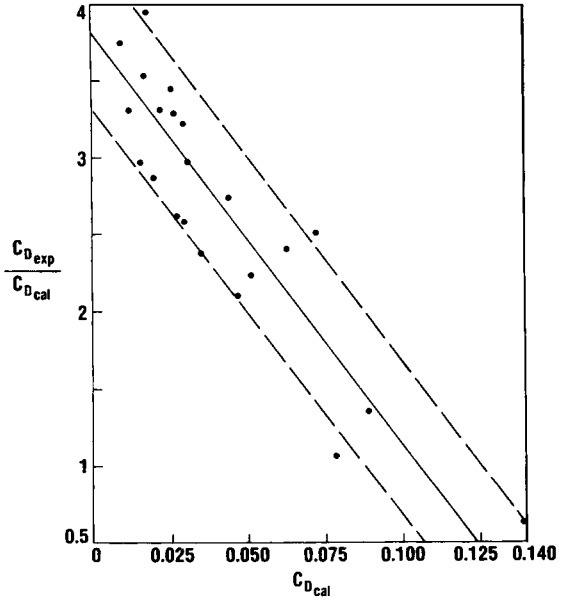

Fig. 9. Correlation of $C_{D_{exp}}/C_{D_{calc}}$ vs $C_{D_{cal}}$.

of drag obtained from the experimental measurement is not compatible with the value of take-up tension reported. The situation points to a further examination of the magnitude of the air drag contributing to the filament tension in spinning.

CONCLUSIONS

1. Experimentally measured air drag on the moving filament in a spinning system is significantly larger than the drag value estimated by the existing theories. The reason for this is believed to be the swaying of filament which makes the effective filament diameter larger than the true diameter.
2. In some of the spinning sutdies in which the existing theories were used to account for the air drag, the drag effect may have been underestimated considerably.

Most of the experimental work was performed by Dietrich Kattermann.

References

1. V. G. Bankar, J. E. Spruiel, and J. L. White, *J. Appl. Polym. Sci.*, **21,** 2135 (1977).
2. A. Ziabicki, *Kolloid-Z.*, **175,** 14 (1961).
3. E. Cernia, W. Conti, and S. Progetti, *J. Appl. Polym. Sci.*, **17,** 3637 (1973).
4. R. R. Lamonte and C. D. Han, *J. Appl. Polym. Sci.*, **16,** 3285 (1972).
5. B. C. Sakiadis, *A.I.Ch.E. J.*, **7**(3), 467 (1961).
6. A. Selwood, Trans. *J. Text. Inst.*, **9,** 20 (1962).
7. B. C. Sakiadis, *A.I.Ch.E. J.*, **7**(2), 221 (1961).
8. K. Pohlhausen, *Z. Angew. Math. Mech.*, **1,** 252 (1921).
9. M. B. Glauert and M. J. Lighthill, *Proc. Roy. Soc. (London)*, **230A,** 188 (1955).
10. F. M. White, *Trans. ASME J. Basic Eng.*, **94,** 200 (1972).
11. G. N. V. Rao, *Trans. ASME J. Appl. Mech.*, **34,** 237 (1967).
12. R. L. Richmond, Ph.D. Thesis, California Institute of Technology, Pasadena, Calif. 1957.
13. Y. S. Yu, *J. Ship Res.* **3,** 33 (1958).
14. T. Cebesi, *Trans. ASME J. Basic Eng.*, **92,** 545 (1970).
15. S. L. Anderson and R. Stubbs, *J. Text. Inst.*, **49,** T53 (1958).
16. T. Ishibashi, K. Aoki, and T. Ishii, *Kobunshi Kagaku*, **27**(300), 211 (1970); *J. Appl. Polym. Sci.*, **14,** 1597 (1970).

Received June 12, 1978